

## Abrasive Waterjet Machining Simulation by Coupling Smoothed Particle Hydrodynamics/Finite Element Method

WANG Jianming<sup>1,2,\*</sup>, GAO Na<sup>1</sup>, and GONG Wenjun<sup>1</sup>

<sup>1</sup> School of Mechanical Engineering, Shandong University, Jinan 250061, China

<sup>2</sup> Key Laboratory of High Efficiency and Clean Mechanical Manufacture of Ministry of Education, Shandong University, Jinan 250061, China

Received May 19, 2009; revised August, 2010; accepted August, 2010; published electronically August, 2010

**Abstract:** In dealing with abrasive waterjet machining(AWJM) simulation, most literatures apply finite element method(FEM) to build pure waterjet models or single abrasive particle erosion models. To overcome the mesh distortion caused by large deformation using FEM and to consider the effects of both water and abrasive, the smoothed particle hydrodynamics(SPH) coupled FEM modeling for AWJM simulation is presented, in which the abrasive waterjet is modeled by SPH particles and the target material is modeled by FEM. The two parts interact through contact algorithm. Utilizing this model, abrasive waterjet with high velocity penetrating the target materials is simulated and the mechanism of erosion is depicted. The relationships between the depth of penetration and jet parameters, including water pressure and traverse speed, etc, are analyzed based on the simulation. The simulation results agree well with the existed experimental data. The mixing multi-materials SPH particles, which contain abrasive and water, are adopted by means of the randomized algorithm and material model for the abrasive is presented. The study will not only provide a new powerful tool for the simulation of abrasive waterjet machining, but also be beneficial to understand its cutting mechanism and optimize the operating parameters.

**Key words:** abrasive waterjet machining, randomized algorithm, coupling SPH/FEM, abrasive material models

### 1 Introduction\*

Abrasive waterjet(AWJ) cutting, due to its various distinct advantages over other cutting technologies, such as no thermal distortion, high machining versatility, high flexibility and small cutting forces, is being increasingly used in various industries<sup>[1]</sup>.

Since AWJ cutting process influenced by several process parameters, such as hydraulic, abrasive, target and cutting parameters, etc, proposing the appropriate modeling for AWJ machining(AWJM) is a heat study field. Both analytical and empirical methods have been used to model the AWJM process<sup>[2]</sup>, including fuzzy logic algorithms<sup>[3]</sup> and reaction kinetics<sup>[4]</sup>. However, both empirical models and heuristic approaches need extensive experimental data, which is a major drawback due to high expense and limited applicability. There are a few literatures focusing on the numerical simulations of the impact process, which often use finite element method(FEM) with a single abrasive to calculate the erosive wear during AWJ machining, and the abrasive was modeled as a rigid ball ignoring the essential material property<sup>[5]</sup>. The modeling with a single abrasive

particle was just the micro-modeling study and couldn't conclude the machining process influence factors and mechanism of the AWJM. Using the FEM method to simulate AWJM process, which is the fluid-solid impact problem and accompanies with large deformation, may lead to the distortion of the mesh and has been discussed in Ref. [6].

To overcome the above-mentioned difficulty, we developed a coupled method of smoothed particle hydrodynamic(SPH) and FEM. The appeal of SPH for high velocity AWJ impact is that it is a meshfree method and belongs to Lagrangian frame, which needn't mesh connectivity so as to allow severe mesh distortions. By SPH method, the continuous material is expressed by a series of particles, which carry some physical quantum, such as mass and velocity. This property is regularly adapted for hydrokinetics problems. JOHNSON, et al<sup>[7-9]</sup>, applied SPH in high velocity impacting problems and got encouraging results. Thus SPH can overcome the defect of FEM and belongs to Lagrangian frame description, and the computation will be more compact and automatic.

Modeling based on coupling SPH and FEM for AWJM simulation is presented in this paper, in which the AWJ is modeled by SPH particles and the target material is modeled by finite elements. The two parts interact by contact algorithm of "nodes-to-surface" in LS-Dyna. The

\* Corresponding author. E-mail: wangjianming@sdu.edu.cn

This project is supported by Shandong Provincial Natural Science Foundation of China (Grant No. Y2007A07)

multi-materials SPH particles modeling, in which the abrasives and water mix together uniformly, is proposed. The randomized algorithm for the actual mass percentage of two materials is used. Based on the explicit program LS-Dyna, the hybrid-code of SPH and FEM is conducted to simulate the machining process, and the simulation results are tested by the experimental data.

The structure of the paper is as follows: in section1, the current situation of researches for the AWJM simulation is surveyed and modeling based on coupling SPH and FEM for AWJM simulation is proposed. In section 2, some basic theories of SPH are described. In section 3, the related theories and algorithms for modeling are expounded, including material models and randomized algorithm, etc. In section 4, some simulation results are revealed and contrastive analysis between the simulation results and experiment data is carried out. At last, some conclusions are educed.

## 2 Basic Theories

### 2.1 Basic theory of SPH

Instead of a grid, SPH uses a kernel interpolation to approximate the field variables at any point in a domain. For instance, an estimate value of a function  $f(x)$  at the location  $x$  is given in a continuous form by an integral of the product of the function and a kernel (weighting) function  $W(x-x', h)$  as follows:

$$\langle f(x) \rangle = \int_{\Omega} f(x') W(x-x', h) dx', \quad (1)$$

where  $\langle f(x) \rangle$ —Kernel approximation,  
 $h$ —Smoothing length,  
 $x'$ —New independent variable.

The kernel function usually has the following properties: compact support, which means that it's zero everywhere but on a finite domain inside the range of the smoothing length  $2h$ :

$$W(x-x', h) = 0 \quad \text{for} \quad |x-x'| \geq 2h. \quad (2)$$

The kernel function is normalized as:

$$\int W(x-x', h) dx' = 1. \quad (3)$$

These requirements ensure that the kernel function reduces to the Dirac delta function when  $h$  tends to zero:

$$\lim_{h \rightarrow 0} W(x-x', h) = \delta(x-x', h). \quad (4)$$

And therefore, Eq. (1) follows that:

$$\lim_{h \rightarrow 0} \langle f(x) \rangle = f(x). \quad (5)$$

If the function  $f(x)$  is only known at  $N$  discrete points, the integral of Eq. (1) can be approximated by a summation:

$$\langle f(x) \rangle = \int_{\Omega} f(x') W(x-x', h) dx' \approx \sum_{j=1}^N \frac{m_j}{\rho_j} f(x_j) W(x-x'_j, h_j), \quad (6)$$

where  $m_j$  and  $\rho_j$  are the mass and density of particle  $j$ , respectively,  $m_j/\rho_j$  is the volume associated to the point  $j$  or particle  $j$ .

Following Eq. (7), one can constitute the basis of SPH method. The value of a variable at a particle, denoted by subscript  $i$ , is calculated by summing the contributions from a set of neighboring particles (Fig. 1), denoted by subscript  $j$  and for which the kernel function is not zero:

$$\langle f(x_i) \rangle = \sum_{j=1}^N \frac{m_j}{\rho_j} f(x_j) W(x_i-x'_j, h_i). \quad (7)$$

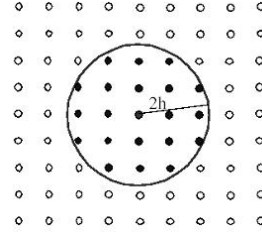


Fig. 1. Set of neighboring particles

### 2.2 Variable smoothing length

If large deformations occur, particles can largely separate from each other. If the smoothing length remains constant, the particle spacing can become so large that particles will no more interact. On the other hand, in compression, a lot of particles might enter in the neighboring domain of each other, which can significantly slow down the calculation. There are many ways to deal with  $h$  so that the number of the neighboring particles remains constant relatively. The simplest approach is to update the smoothing length according to the averaged density as follows:

$$h = h_0 \left( \frac{\rho_0}{\rho} \right)^{\frac{1}{d}}, \quad (8)$$

where  $h_0$  is the initial smoothing length,  $\rho_0$  is the initial density,  $\rho$  is the current density,  $d$  is the number of dimensions of the problem.

Another method to evolve the smoothing length, which takes the time derivative of the smoothing function in terms of continuity equation, is as follows:

$$\frac{dh}{dt} = -\frac{1}{d} \frac{h}{\rho} \frac{d\rho}{dt}. \quad (9)$$

Eq. (9) can be discredited by using the SPH approximations and calculated with the other differential equations in particles.

### 3 Modeling Description

An AWJ impacting a ductile metal plate will be modeled and simulated to investigate the machining mechanism and parameters' influence, including jet velocity and traverse speed, etc. The model parameters are from the experimental data to be convenient for comparisons<sup>[10]</sup>. The target was a 3D metallic block (Carbon steel AISI 1018). The AWJ cutting condition is listed in Table 1. In this section, modeling method, material models and SPH particles modeling for two kinds of materials are discussed.

**Table 1. AWJ cutting condition**

Parameter	Value
Waterjet pressure $p/\text{MPa}$	100–350
Waterjet nozzle $d_n/\text{mm}$	0.33
Traverse rate $u/(\text{mm} \cdot \text{min}^{-1})$	23
Abrasive flow rate $m_a/(\text{g} \cdot \text{s}^{-1})$	2.56
Stand o distance $S/\text{mm}$	3
Abrasive mesh No.(garnet) $n$	80
Mixing tube diameter $d_m/\text{mm}$	1.02

#### 3.1 Modeling method

The coupling SPH/FEM method is used for abrasive waterjet machining simulation. The abrasive waterjet is modeled by SPH particles and the target material is modeled by finite elements. SPH can be seen as a special element and is embedded by “ELEMENT\_SPH” in LS-Dyna, where the SPH element is controlled by node (particle) number and node (particle) mass, and the two parts are interacted by contact algorithm. The particle force imposes on the surface of finite elements by contact type of “CONTACT\_ERODING\_NODES\_TO\_SURFACE” in LS-Dyna, where the slave part is defined with SPH particles and the master part is defined with finite elements. However, the difficulty of the SPH particles modeling is that it contains two kinds of material particles, abrasive and water, so a new algorithm is proposed to resolve the problem in the following subsection.

#### 3.2 Material models

##### 3.2.1 Water material models

The modeling for water is based on an SPH formulation of movement. The water material model leads to the selection of the null-material model in LS-Dyna, which allows equation of state to be considered without computing deviatory stresses and accord with the hydrodynamic behavior laws. We use the Mie-Grueisen equation of state for the water material models as follows:

$$p = \frac{\rho_0 C^2 \mu \left[ 1 + \left( 1 - \frac{\gamma_0}{2} \right) \mu - \frac{a}{2} \mu^2 \right]}{\left[ 1 - (S_1 - 1) \mu - S_2 \frac{\mu_2}{\mu + 1} - S_3 \frac{\mu^3}{(\mu + 1)^2} \right]} + (\gamma_0 + a \mu) \quad (10)$$

Table 2 shows the values of the coefficients in Eq. (10)<sup>[11]</sup>.

**Table 2. Values of the coefficients in Mie-Grueisen equation used for water**

Parameter	Value
Velocity of sound $C/(\text{m} \cdot \text{s}^{-1})$	1 480
Gruneisen gamma $\gamma_0$	0.493 4
Volume correction $a$	1.397
Coefficient $S_1$	2.56
Coefficient $S_2$	-1.986
Coefficient $S_3$	0.228 6
Density $\rho_0/(\text{kg} \cdot \text{m}^{-3})$	1 000

##### 3.2.2 Abrasive material models

The modeling for the abrasive is also based on an SPH formulation of movement. The null-material model is used for abrasive material too. Considering the material behavior of abrasive, we propose the linear polynomial equation of state, which defines the relationship between pressure and density, and the equation of state comes from Refs. [12].

The relationship between  $p$  and  $\rho$  is defined as<sup>[11]</sup>

$$p = C_0^2 (\rho - \rho_{\text{mix}}), \quad (11)$$

where  $C_0$ — Speed of sound of solid abrasive,

$\rho_{\text{mix}}$ — Initial abrasive density which includes some moisture,

$\rho$ — Current abrasive density which includes some moisture.

And

$$\rho_{\text{mix}} = (1 - \alpha_0) \rho_a + \alpha_0 \rho_m, \quad (12)$$

$$\alpha_0 = \frac{V_m}{V}, \quad (13)$$

where  $\rho_a$ — Density of solid abrasive,

$\rho_m$ — Density of moisture,

$V_m$ — Volume of the moisture,

$V$ — Total volume.

Transform Eq. (11) to the form of the linear polynomial equation of state, which is expressed as

$$p = a_1 \mu + a_2 \mu^2 + a_3 \mu^3 + (b_1 \mu + b_2 \mu^2 + b_3 \mu^3) \rho_0 e, \quad (14)$$

where  $a_i$  and  $b_i$  are the polynomial equation coefficients,  $e$  is initial internal energy per unit volume. And

$$\mu = \frac{\rho}{\rho_{\text{mix}}} - 1. \quad (15)$$

Substituting Eq. (15) into Eq. (11), we can gain the final linear polynomial equation of state for the abrasive as follows:

$$p = C_0^2 \rho_{\text{mix}} \mu, \quad (16)$$

where  $C_0$  is equal to 9.03 km/s and can be obtained from Ref. [13].

### 3.2.3 Target material models

The metallic target is considered as kinematic hardening model, whose property parameters are listed in Table 3.

**Table 3. Material properties for the target**

Parameter	Value
Material density $\rho/(\text{kg} \cdot \text{m}^{-3})$	7 860
Elasticity module $E/\text{GPa}$	210
Poisson's coefficient $\nu$	0.284
Yield stress $\sigma_v/\text{MPa}$	260
Tensile strength $\sigma_b/\text{MPa}$	350
Failure strain $\varepsilon$	0.33

In numerical simulation, the removal of elements is used to imitate the crack growth and material failure, and the criterion of material failure is specified in the material model. To the plastic hardening model for target, the plastic failure strain is set as a criterion to examine the probable damaged zone. The strategy was also adopted in Ref. [14].

### 3.3 SPH particles modeling for two kinds of materials using the randomized algorithm

The mass and density of SPH particles are imported to the equation of kernel approximation, which makes the SPH particles have the material property<sup>[15]</sup>. To modeling the two materials of abrasive and water, the actual mass percentage of two materials in the SPH particles' modeling is the key point. A new way to achieve the particles' modeling is proposed in this paper. Firstly, the volumetric flow rates of the abrasive and water according to their mass flow rate are calculated; secondly, basing on the volumetric flow rates of the two materials, the volume percentages of the each material can be achieved; finally, the randomized algorithm is utilized to realize the percentage of two kinds of SPH particle numbers and their distribution. At the same time, each density can be given. With their particle numbers and density, the SPH particles including two kinds of materials properties are established, which can be seen in Fig. 2. The blue particles denote the materials of abrasive and the green ones represent to the water.

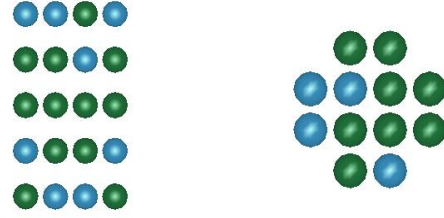


Fig. 2. SPH particles for different materials determined by randomized algorithm

## 4 Simulation, Numerical Results and Discussions

According to the experiment conditions<sup>[10]</sup>, the carbon steel AISI 1018 is chosen as the work piece material for the experiments. The dimensions of each sample are: 100 mm in length, 13 mm in width, and 65 mm in height. The AWJ conditions used in this study are listed in Table 1. A model for AWJM is created and its simulation results are compared with the experiment to validate the correction of the modeling. The modeling method has depicted in section 3, the AWJ is modeled by SPH particles with abrasive and water, the target material is modeled by finite elements, which is shown in Fig. 3(a). Figs. 3(b), 3(c), 3(d) are the simulation results at different time under the pressure 100 MPa.

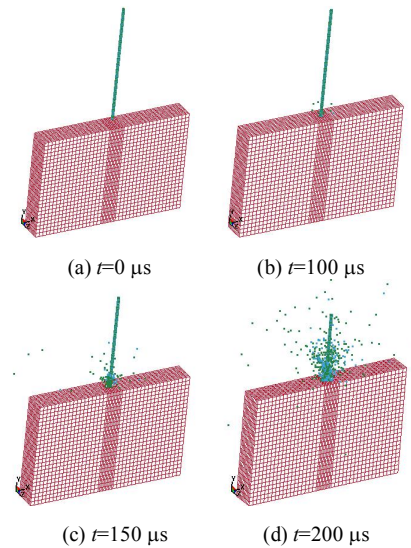


Fig. 3. AWJ simulation results at different time

The AWJ has the diameter of 1.02 mm and the height of 76 mm, the stand-off distance far from the target is 3 mm. There are a total of 2 399 SPH particles in the waterjet model. The diameter of single SPH particle is determined according to abrasive size in the experiment. The amount and distribution of SPH particles are determined by the randomized algorithm. The target model is in the size of  $100 \times 13 \times 65 \text{ mm}^3$ , meshed by 8-nodes brick element, the number of elements is 11 960 with the nodes of 30 184. The non-reflecting conditions are adopted on the boundaries of target to eliminate the reflection of stress

waves, by which the infinite boundary conditions can be satisfied. The SPH particles and target's elements are interacted by contact algorithm. The initial velocity of SPH particles,  $V_e$  is determined according to the waterjet pressure  $p$ , varying from 100 to 350 MPa in Table 1, the relationship between  $V_e$  and  $p$  is shown in Fig. 4.  $V_e$  is an important parameter for the model and can be approximated by the momentum transfer equation between incoming and exit of AWJ nozzle<sup>[16-17]</sup>. The traverse speed  $u$  is given as another initial velocity.

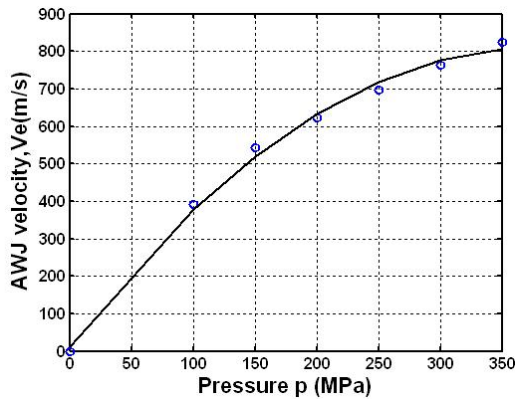


Fig. 4. Relationship between the AWJ velocity and the pressure

Fig. 5 shows the centric cross sections of the impact area at different time under the pressure 100 MPa. The plastic deformation was found to be very localized in the impact area. It shows that the depth of cut increases as the time increasing. As a result, the plastic deformation, in the form of crater, significantly increased up to its maximum depth at the time  $t=255 \mu\text{s}$ .

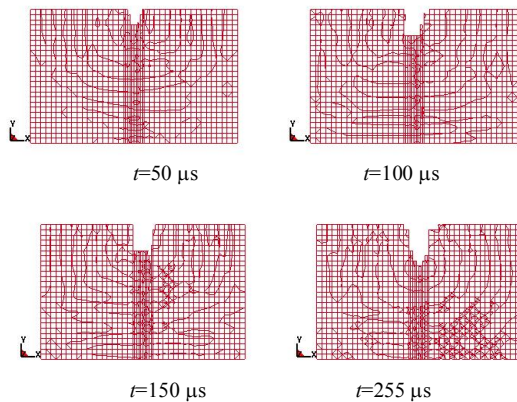


Fig. 5. Erosion process in the centric cross section of target

Fig. 6 shows the effect of the pressure on the cut depth in AWJM. In general, the depth of penetration increases with water pressure, as more energy will be able to remove more material. Study from Ref. [18] finds that this increase is almost in a linear form at initial stage, and as the water pressure further increases, the rate of increase declines. This is due to the fact that a higher water pressure tends to

open a wider kerf which will have a negative effect on the depth of penetration. Compared with the experimental data<sup>[10]</sup>, the simulation results appear to be able to represent this trend very well at water pressure up to 250 MPa. It also shows a good agreement with the experimental data at the water pressure up to 350 MPa though it overestimates the depth of penetration in some cases. Thus, the model can be considered to be valid by experimental data for water pressure from 100 to 350 MPa.

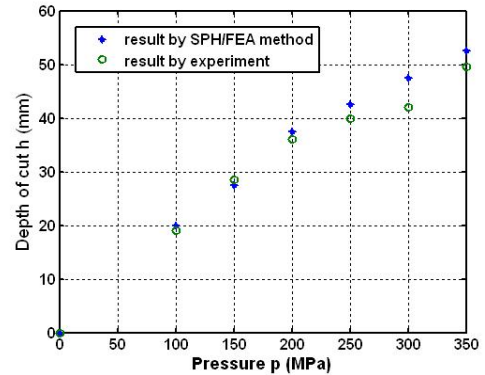


Fig. 6. Variation of cut depth with pressure

In order to study the influence of the traverse rate, we build another model based on the experimental data from Ref. [19], which is similar to the experiment from Ref. [10] except the abrasive mass flow rate and jet traverse speed.

Fig. 7 shows that the depth of penetration decreases with an increase of jet traverse rate. This is due to a number of factors. Firstly, as the traverse speed increases, the number of particles impinging on a given exposed target area decreases, which in turn reduces the material removal rate. Secondly, MOMBBER, et al<sup>[20]</sup>, found that the effects of damping and friction on the jet decreased as the jet exposure time decreased (or the jet traverse rate increased). Thus, an increase in the jet traverse speed will reduce the energy loss of the particles and improve the material removal rate. Thirdly, it has been reported that with a faster travel of the jet, fewer particles will be able to strike on the target material and open a narrower slot<sup>[18]</sup>. Consequently, as a result of the reducing energy loss and the narrowing kerf width at a high traverse speed, the decline rate of the penetration depth will reduce and the curves in the graphs tend to flattening as the traverse speed increases.

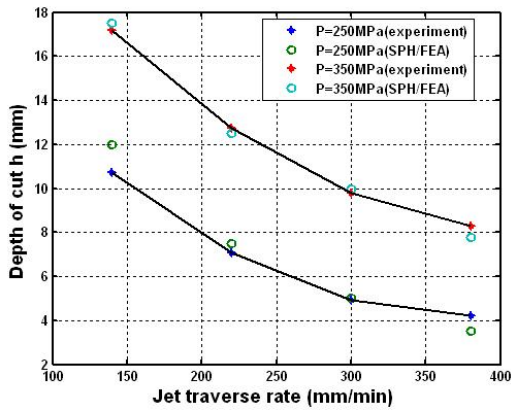


Fig. 7. Relationship between jet traverse rate and the depth of penetration when  $m_a=0.45$  kg/min

## 5 Conclusions

(1) This paper presents a coupling SPH/FEM method to simulate the abrasive waterjet machining. The model deals with fluid–solid interaction. Material models of abrasive are proposed, and the SPH particle modeling for two kinds of material is also proposed. The AWJM is simulated successfully.

(2) Based on the test data, the model has been shown to be able to provide adequate estimation of the cutting performance for ductile metal under pressure range of 100–350 MPa and may be used for process control as well as optimization for the operating parameters.

(3) The good agreement between simulation results and the experimental data has confirmed the correctness and credibility of the model.

## References

- [1] VAN LUTTERVELT C A. On the selection of manufacturing methods illustrated by an overview of separation techniques for sheet materials[J]. *Annals of the CIRP*, 1989, 38(2): 587–607.
- [2] VENKATESH V C. Parametric studies on abrasive jet machining[J]. *Annals of the CIRP*, 1984, 33(1): 109–112.
- [3] KOVACEVIC R, FANG M. Modeling the influence of the abrasive waterjet cutting parameters on the depth of cut based on fuzzy rules[J]. *International Journal Machine Tools and Manufacture*, 1994, 34(1): 55–72.
- [4] MOMBER A W. A generalized abrasive water jet cutting model[C]// *Proceedings of the 8th American Water Jet Conference*, St. Louis, MO, August 26–29, 1995: 359–376.
- [5] ELTOBGY M S, NG E, ELBESTAWI M A. Finite element modeling of erosive wear[C]. *International Journal of Machine Tools and Manufacture*, 2005, 45:1337-1346.
- [6] MA Li, BAO Ronghao, GUO Yimu, Waterjet penetration simulation by hybrid code of SPH and FEA[J]. *International Journal of Impact Engineering*, 2008, 35(9): 1 035–1 042.
- [7] JOHNSON G R, BSISSEL S R. Normalized smoothing functions for SPH impact computations [J]. *Int. J. Numer. Math. Eng.*, 1996, 39(2): 2 725–2 741.
- [8] JOHNSON G R, STRYK R A. BSISSEL S R. SPH for high velocity impact computations[J]. *Comput. Methods Appl. Mech. Eng.*, 1996, 139: 347–373.
- [9] JOHNSON G R, BSISSEL S R, STRYK R A. Generalized particle algorithm for high velocity impact computations[J]. *Comput. Mech.*, 2000, 25: 245–256.
- [10] ASHRAF I HASSAN, CHEN C, KOVACEVIC R. On-line monitoring of depth of cut in AWJ cutting[J]. *International Journal of Machine Tools and Manufacture*, 2004, 44(6): 595–605.
- [11] STEINBERG D J. Spherical explosions and the equation of state of water[R]. *Lawrence Livermore National Laboratory, Livermore, CA*, 1987.
- [12] GRUJICIC M, PANDURANGAN B, QIAO R, et al. Parameterization of the porous-material model for sand with different levels of water saturation[J]. *Soil Dynamics and Earthquake Engineering*, 2008, 28(1): 20–35.
- [13] GWANMESIA G D, ZHANG J, DARLING K, et al. Elasticity of polycrystalline pyrope ( $Mg_3Al_2Si_3O_{12}$ ) to 9GPa and 1000°C[J]. *Physics of the Earth and Planetary Interiors*, 2006, 155(3–4): 179–190.
- [14] BITTER J G A. A study of erosion phenomena: Part I [J]. *Wear*, 1993, 6: 5–21.
- [15] LIU G R, LIU M B. *Smoothed particle hydrodynamics*[M]. Singapore: World Scientific publishing Co. Ltd., 2005.
- [16] EITobgy M, NG E G. Modeling of abrasive waterjet machining: a new approach[J]. *CIRP Annals-Manufacturing Technology*, 2005, 54(1): 285–288.
- [17] HASHISH M. Pressure effects in abrasive water jet (AWJ) machining[J]. *Journal of Engineering Materials and Technology*, 1993, 11: 221–228.
- [18] WANG J. Abrasive waterjet machining of polymer matrix composites — cutting performance, erosive process and predictive models[J]. *J. Adv. Manuf. Technol.*, 1999, 15: 757–768.
- [19] PAUL S, HOOGSTRATE, A M LUTTERWELT, et al. Analytical and experimental modeling of abrasive water jet cutting of ductile materials[J]. *Journal of Materials and Processing Technology*, 1998, 73: 189-99.
- [20] MOMBER A W, MOHAN R S, KOVOVACEVIC R. On-line analysis of hydro-abrasive erosion of pre-cracked materials by acoustic emission[J]. *Theoret. Appl. Fract. Mech.*, 1999, 31: 1–17.

## Biographical notes

WANG Jianming, born in 1962, is currently a professor in School of Mechanical Engineering, Shandong University, China. He received his PhD degree from School of Mechanical Engineering, Tianjin University, China, in 1997. His research interests include computational mechanics, meshfree methods, multibody system dynamics and waterjet machining.

Tel: +86-531-88392261; E-mail: wangjianming@sdu.edu.cn

GAO Na, born in 1985, is currently a master candidate in School of Mechanical Engineering, Shandong University, China. E-mail: gaoxiaodou0116@hotmail.com.cn

GONG Wenjun, born in 1983, is currently a master candidate in School of Mechanical Engineering, Shandong University, China. E-mail: gwjagassi@yahoo.com.cn